Anti-corrosion protection of steel with superhydrophobic coatings based on nickel and zinc

L.E. Tsygankova,[1]* L.D. Rodionova,[1] A.A. Uryadnikov[1] and N.V. Shel[2]

[1]*Derzhavin State University, ul. Internatsyonalnaya, 33, 392000 Tambov, Russian Federation*
[2]*Tambov State Technical University, ul. Sovetskaya, 106, 392000 Tambov, Russian Federation*
**E-mail: vits21@mail.ru*

Abstract

Two types of suprehydrophobic (SHP) coatings with contact angles of 153±2° and 155±3° were obtained on St3 carbon steel by electrodeposition of nickel and zinc respectively followed by exposure to an ethanol solution of myristic acid. Their protective effectiveness was studied at 100% humidity, in distilled water, in gas and liquid phases of SO_2 solutions (1 and 3%) for 10 days, in a sodium chloride solution (50 g/L) for 168 hours, in a salt fog chamber before the first signs of corrosion appear. The methods of gravimetry, potentiodynamic polarization, impedance spectroscopy, scanning electron microscopy, and contact angle measurements were used. After testing at 100% humidity and in distilled water, the state of the SHP coatings remained virtually unchanged. In both phases of solutions with 1% SO_2 and in the gas phase of 3% SO_2 solution, the SHP coatings were degraded to some extent, although hydrophobicity was retained, as in the NaCl solution. The protective properties of SHP coatings based on Zn were shown to have a superiority to Ni-based SHP coatings.

Received: July 4, 2024. Published: July 22, 2024 doi: 10.17675/2305-6894-2024-13-3-11

Key words: *steel protection, superhydrophobicity, nickel, zinc, myristic acid, sulfur oxide, sodium chloride, contact angle.*

Introduction

Over the past two decades, extensive research has been carried out on the anti-corrosion properties of superhydrophobic coatings (SHPCs) on metals. Superhydrophobic coatings include those with a water contact angle of ≥150°. The main conditions for obtaining SHP coatings are the creation of multimodal roughness, which allows air bubbles to be trapped in micropores, preventing the penetration of liquid to the substrate, and the application of hydrophobic agents with low surface energy to the surface. Carboxylic acids with a long hydrocarbon radical, fluorocarbons, fluoroxysilanes, *etc*. are used as such. Various methods for producing superhydrophobic coatings, as well as methods for assessing their anti-corrosion properties, have been developed. Methods of laser processing of a metal surface

to create multimodal roughness with subsequent application of a fluorine-containing hydrophobic agent to the surface are very effective [1, 2]. These are expensive methods. In addition to them, a number of cheaper methods are proposed, based on the electrochemical deposition of the same metals or another metals with simultaneous or subsequent treatment with an ethanol solution of stearic or myristic acids. Thus, in [3], the SHP coating was obtained on low-carbon steel by cathodic deposition of nickel from a solution of $NiCl_2 \cdot 6H_2O$ (200 g/L)+H_3BO_3 (30 g/L)+KCl (30 g/L) with subsequent exposure of the sample to 0.1 M ethanol solution of myristic acid for an hour at room temperature. The resulting coating with a contact angle of 152.6° was characterized by mechanical stability. Its anti-corrosion properties were studied by potentiodynamic polarization and impedance spectroscopy methods in a 3.5% NaCl solution immediately after receiving the coating and establishing a stable potential. According to the data obtained, the corrosion current in the presence of the SHP coating decreased by 28 times. Long-term studies of anti-corrosion properties have not been carried out. In [4], the SHP coating on steel was obtained by cathodic deposition of nickel from a 0.5 M $NiSO_4$ solution at a current density of 60 A/dm^2, followed by exposure to a 0.02 M stearic acid solution for 1 min. The contact angle was 154.4°, the rolling angle was 2°. The anticorrosion properties of the resulting SHP coating were assessed in a 3.5% NaCl solution using potentiodynamic polarization. The corrosion current on the sample with SHP coating was $2.05 \cdot 10^{-5}$ mA/cm^2 and was approximately 3 times lower than on the sample without coating.

Authors of [5] describe the preparation of a SHP coating on iron by cathodic deposition of zinc from a solution of 0.01 M $Zn(CH_3COO)_2$+0.1 M NaCI+0.1 M HCl at a potential of –1.8 V for 1100 s, followed by annealing at 180°C for 70 min. Annealing made it possible to obtain a superhydrophobic coating with a contact angle of 163±2° and a rolling angle of 0±2°. When stored in air at room temperature for a year, the contact angle remained within the range of 162–166º. The anticorrosion properties of the coating were studied using the potentiodynamic polarization method. The corrosion current on the sample coated was an order of magnitude less than on the iron sample uncoated, and 2 orders of magnitude less than on pure zinc. Long-term studies on anti-corrosion behavior have not been carried out. In [6], SHP zinc coating was obtained on samples of pipe steel by cathodic deposition of zinc from a solution of $ZnSO_4 \cdot 7H_2O$ (240 g/L), acidified to pH=4 with sulfuric acid (with a Zn anode) with sequential application of a current density of 4 A/dm^2 and 9 A/dm^2, followed by treatment in a 0.01 M ethanol solution of perfluorooctanoic acid for 11 days at room temperature. The contact angle on the resulting superhydrophobic Zn coating was 154.2°, and the rolling angle was less than 5°. The contact angle, according to the authors, remained greater than 150° when stored in air for 80 days. Anti-corrosion studies of the coating have not been carried out. The authors of [7] achieved superhydrophobicity of X90 pipe steel plates by cathodic deposition of a Cu–Zn coating from a solution of $ZnSO_4 \cdot 7H_2O$+$CuSO_4 \cdot 5H_2O$ (0.169 M)+$C_4O_6H_4KNa \cdot 4H_2O$ (100 g/L)+NaOH (50 g/L) with a brass anode without the use of a low surface energy modifier. Different Zn^{2+}/Cu^{2+} ratios were used. The coatings obtained after electrodeposition were hydrophilic. However, after

exposure to air for more than 60 days, they acquired superhydrophobicity with a contact angle of 154.73° and a roll-off angle of about 6.5°. The authors explain the appearance of superhydrophobicity by the formation of CuO and ZnO oxides, as well as the adsorption of oxygen. Superhydrophobicity was retained, *i.e.* the contact angle practically did not change when drops of liquid with different pH values from 1 to 13 were applied to the surface. Superhydrophobicity was also maintained when samples with coating were kept in water for 5 hours, as well as at elevated temperatures up to 200°C for 9 hours. The anticorrosion properties of the resulting SHP coating were assessed using potentiodynamic polarization in a 3.5% NaCl solution. The corrosion current density for the sample coated was $4.3115 \cdot 10^{-7}$ A/cm^2, and for the sample without coating it was $1.4637 \cdot 10^{-6}$ A/cm^2. According to the authors, electrochemical testing of the SHP coating did not lead to a loss of superhydrophobicity; the contact angle remained greater than 150°. The coating also demonstrates good self-cleaning properties from dirt.

An important issue from a practical point of view is the durability of the anti-corrosion properties of superhydrophobic coatings. In most studies, as discussed above, the protective effectiveness of such coatings is assessed after 0.5 or 1 hour exposure, most often to a sodium chloride solution, according to polarization or impedance measurements. In rare cases, gravimetric corrosion measurements are carried out.

The purpose of this study was to obtain superhydrophobic coatings based on nickel and zinc on St3 steel and to study their anti-corrosion effectiveness under different conditions.

Experimental

Superhydrophobic coatings on St3 steel were obtained through two-stage processes: in the first stage, nickel or zinc was electrodeposited on the surface of a steel plate with dimensions of 30×40×0.7 mm; in the second stage, the plates coated were kept for 1 hour in a 0.1 M ethanol solution of myristic acid. The samples used were St3 steel with composition, mass. %: C – 0.28; Mn – 0.70; Si – 0.15; P – 0.04; S – 0.05; Cr – 0.30; Ni – 0.20; Cu – 0.20, the rest Fe.

Before electrodeposition, the steel plate was ground and degreased with acetone, kept for 30 s in a 0.4 M H_2SO_4 solution to remove the oxide layer, washed with distilled water and placed in an electrolytic bath as a cathode; a platinum plate served as the anode.

Electrodeposition of nickel was carried out in a solution of $NiSO_4 \cdot 7H_2O$ (140 g/L) at a current density of 30 A/m^2 for 5 minutes at room temperature with a nickel anode. Next, the plate with electrodeposited nickel was washed with distilled water, dried in air, and placed in a 0.1 M ethanol solution of myristic acid. After holding for an hour, the plate was removed from the solution, washed with distilled water, dried and left in air for 2 weeks.

Electrodeposition of zinc on a steel plate was carried out in a solution of $ZnSO_4 \cdot 7H_2O$ (0.84 M) with pH=4 under the following conditions: current density 0.4 A/dm^2 for 15 min, then 0.9 A/dm^2 for 2 min at room temperature with zinc anode. Subsequent processing was the same as for obtaining Ni coating.

After exposure to an ethanol solution of myristic acid, the contact angle Θ on samples with Ni coating averaged 146°, and with Zn coating 142.2°. After two weeks of exposure to air, the contact angles increased to 153±2° and 155±3°, respectively. These data confirm the phenomena of the occurrence or increase of superhydrophobicity described in the literature when exposed to air [8–10]. The authors of [8, 9] confirmed by X-ray analysis the adsorption of fragments with C–C–, C–H, C–O– and C–O–C bonds from the air on the surface, which contributes to its hydrophobization.

A scanning electron microscope (JSM 6390, JEOL, Japan and JCM-7000. JEOL Japan 2021) was used to evaluate the condition of the coating. Contact angles were measured at 9 different points on the surface by applying 3–4 μL drops of distilled water using a tensiometer (Easy Drop, KRUSS, Germany). The degradation of superhydrophobic coatings is accompanied by a decrease in the static contact angle Θ, so the stability of the coating can be judged based on the change in Θ over time.

The protective effectiveness of the resulting SHP coatings was studied at room temperature for 240 hours (10 days) under conditions of 100% humidity, in distilled water, in the gas and liquid phases of SO_2 solutions (1 and 3 wt.%), as well as in a NaCl solution (50 g/L) and salt fog chamber. The magnitude of the protective effect (Z, %) of coatings was calculated using the formulas:

$$Z, \% = 100(K_0 - K_{SHPC})/K_0 \quad (1)$$

$$Z, \% = 100(i_0 - i_{SHPC})/K_0 \quad (2)$$

where K_0(i_0) and K_{SHPC}(i_{SHPC}) are the rates (current densities) of corrosion in the absence and presence of SHP coating, respectively. The values of K_0 and K_{SHPC} were determined by the gravimetric method, and i_0 and i_{SHPC} were determined on the basis of polarization curves by extrapolating their Tafel sections to the corrosion potential. Potentiodynamic (0.66 mV/s) polarization measurements were carried out using an IPC-Pro potentiostat (produced at A.N. Frumkin Institute of Physical Chemistry and Electrochemistry, RAS). The potentials were measured with respect to the saturated silver/silver chloride electrode and were recalculated to the standard hydrogen scale. The counter electrode is a smooth platinum.

The impedance spectra were studied according to the method described in [11] using an electrochemical measuring complex from Solartron (UK), consisting of an SI 1255 impedance analyzer and an SI 1287 potentiostat.

Results and Discussion

The morphology of the coating obtained on a steel electrode by electrodeposition of nickel, exposure to a solution of myristic acid and subsequent exposure to air for 2 weeks is shown in Figure 1.

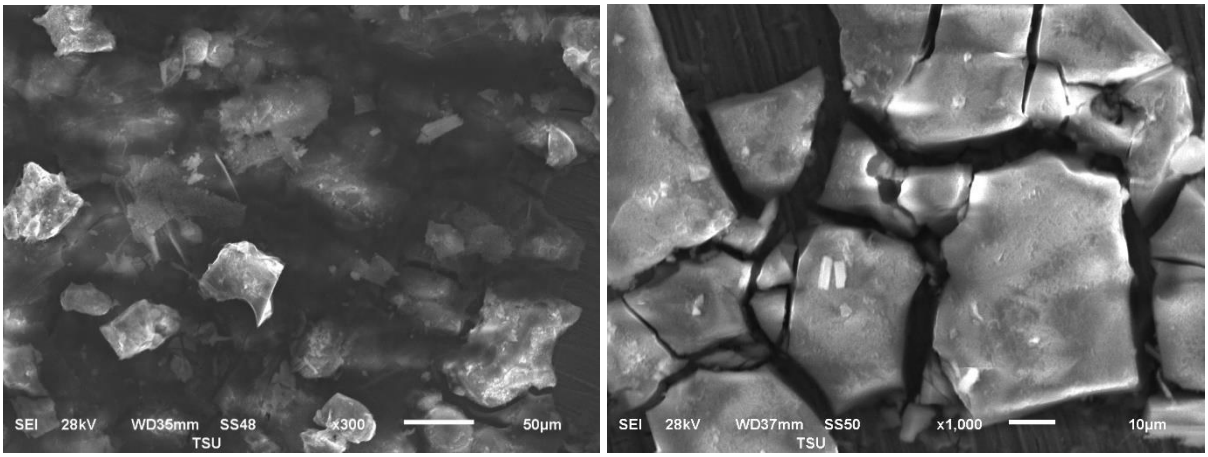

a **b**

Figure 1. SEM image of the superhydrophobic surface obtained on a steel electrode by electrodeposition of nickel.

Large formations up to 50 μm in size and much smaller ones are visible on the surface, which indicate multi-level surface roughness. The presence of grooves helps to capture the air bubbles by them, preventing the penetration of liquid to the metal surface. The interaction of myristic acid with the freshly formed Ni coating helps to reduce the surface energy.

The morphology of the superhydrophobic coating with electrodeposited zinc is shown in Figure 2, on which particles of different sizes are recorded. Needle-like structures covering large-sized particles are visible.

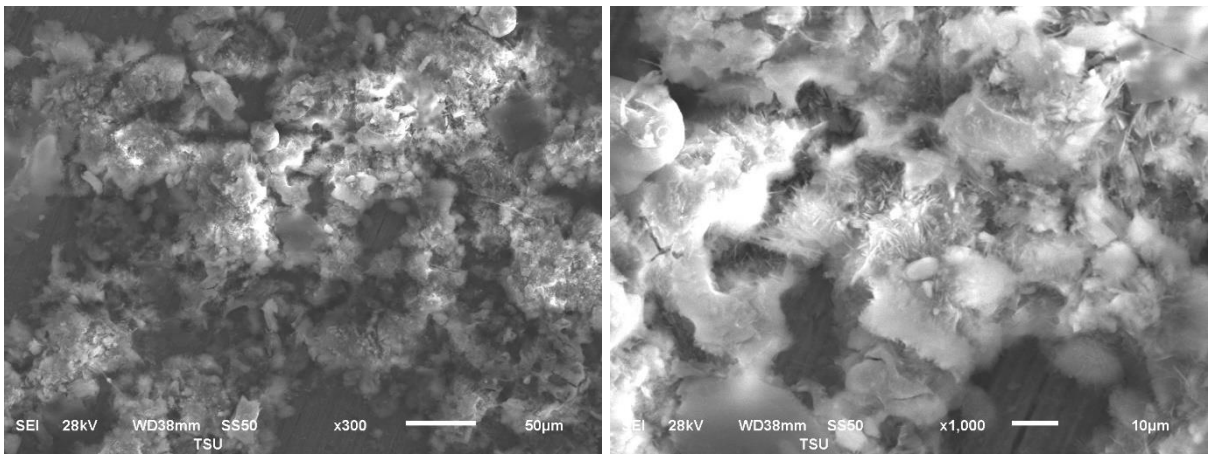

a **b**

Figure 2. SEM image of the superhydrophobic surface obtained on a steel electrode by electrodeposition of zinc.

Figures 3 and 4 show the spectra of SHP coatings based on Zn and Ni, the elemental composition of which confirms the modification of the surface in a solution of myristic acid.

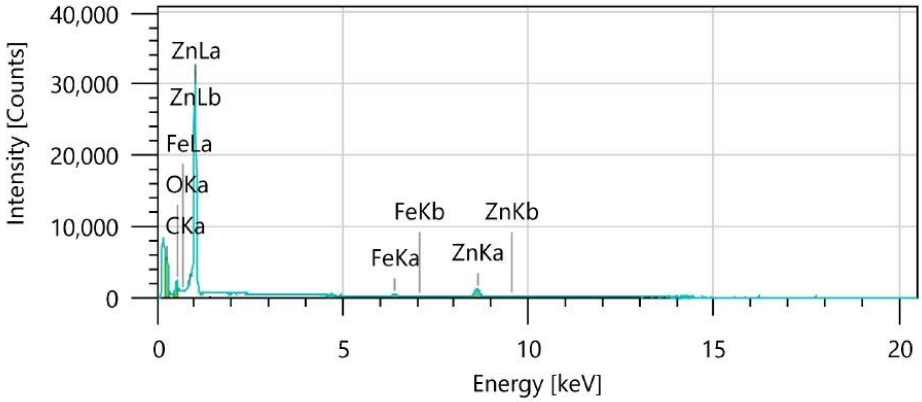

Display name	Standard data	Quantification method	Result Type
Spc_007	Standardless	ZAF	Metal

Element	Line	Mass%	Atom%
C	K	30.49±0.35	61.91±0.72
O	K	10.35±0.27	15.78±0.41
Fe	K	3.61±0.20	1.58±0.09
Zn	K	55.55±1.37	20.73±0.51
Total		100.00	100.00

Figure 3. Spectrum of a zinc-based superhydrophobic coating and its elemental composition.

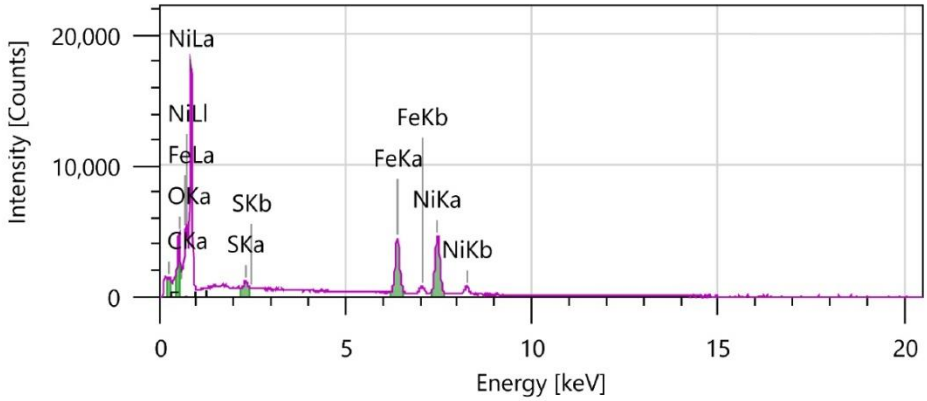

Display name	Standard data	Quantification method	Result Type
Spc_004	Standardless	ZAF	Metal

Element	Line	Mass%	Atom%
C	K	1.96±0.06	7.67±0.24
O	K	5.74±0.11	16.83±0.31
S	K	0.69±0.03	1.01±0.05
Fe	K	31.27±0.40	26.27±0.34
Ni	K	60.34±0.75	48.23±0.60
Total		100.00	100.00

Figure 4. Spectrum of a Ni-based superhydrophobic coating and its elemental composition.

Exposure of steel samples with superhydrophobic coatings of both types under conditions of 100% humidity for 10 days led to a slight change in the contact angle, and subsequent exposure to air for 28 days contributed to achieving almost the same value of Θ (Table 1). There were no mass losses of the sample during the experiment. Images of water droplets before and after the experiment are shown in Figure 5 and 6.

Table 1. Contact angles of SHP coatings on steel: Θ_1 – initial, Θ_2 – after 10 days in conditions of 100% humidity, Θ_3 – after 28 days in air.

Type of coating	Θ_1	Θ_2	Θ_3
Ni-based SHPC	153	151.7	152.7
Zn-based SHPC	155.2	153.5	154

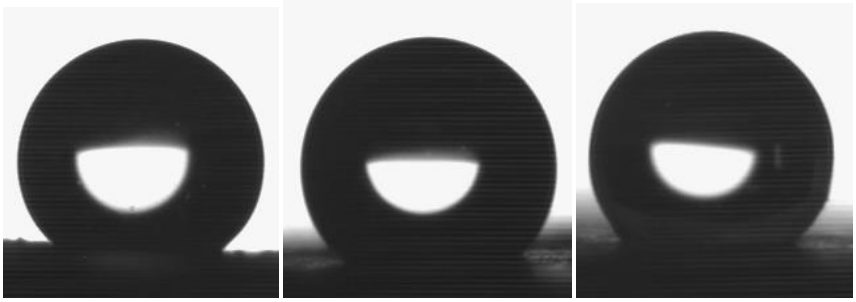

a **b** **c**

Figure 5. Image of water droplets on a Ni-based SHP coating: a – initial – 153°; b – after 10 days of holding the samples at 100% humidity – 151.7°; c – after exposure to air – 152.7°.

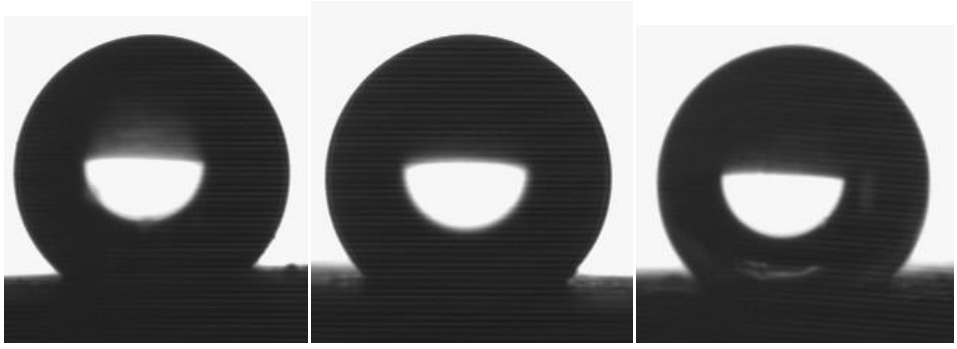

a **b** **c**

Figure 6. Image of water droplets on a Zn-based SHP coating: a – initial – 155.2°; b – after 10 days of holding the samples at 100% humidity – 153.5°; c – after exposure to air – 154°.

Keeping samples with a superhydrophobic coating in distilled water for 10 days, as well as under conditions of 100% humidity, did not lead to a significant decrease in the contact angles (Table 2). There were no mass losses of the sample. The appearance of the coatings has not changed.

Table 2. Average values of contact angles on steel plates with a superhydrophobic coating: Θ_1 – initial, Θ_2 – after 10 days in distilled water, Θ_3 and Θ_4 – after 28 and 35 days in air respectively.

Type of coating	Θ_1	Θ_2	Θ_3	Θ_4
Ni-based SHPC	152	150.7	150.9	151.1
Zn-based SHPC	156	153.8	154.4	154.2

Thus, keeping steel samples with the superhydrophobic coatings studied under conditions of 100% humidity and in distilled water for 10 days does not lead to noticeable changes in the state of the SHP coating.

Tests of the SHP coatings studied in the liquid and gas phases of SO_2 solutions were carried out due to the fact that this sulfur oxide is present in almost any atmosphere: $MPC_{a.d.}=0.05$ mg/m^3, $MPC_{w.z.}=10$ mg/m^3 [12]. Large concentrations of SO_2 in the air are observed in factory atmospheres, near industries associated with metal sulfides. The corrosive aggressiveness of SO_2 with respect to metals is especially pronounced at high air humidity, which is associated with acidification of the medium and its participation as a cathode depolarizer.

SO_2 reacts with water to form sulfurous acid, which dissociates in two steps:

$$SO_2 + H_2O \leftrightarrow H_2SO_3 \quad (3)$$

$$H_2SO_3 \overset{K_a^I}{\leftrightarrow} H^+ + HSO_3^- \quad (4)$$

$$HSO_3^- \overset{K_a^{II}}{\leftrightarrow} 2H^+ + SO_3^{2-} \quad (5)$$

$K_a^{\mathrm{I}} = 1.7 \cdot 10^{-2}$, $K_a^{\mathrm{II}} = 6.8 \cdot 10^{-8}$ [13]. Due to the solubility of SO_2 in water, its initial and equilibrium concentrations will differ. Moreover, their values, as well as the concentrations of hydrogen ions, sulfurous acid and products of its electrolytic dissociation, depend on the ratio V_{gas}/V_{liquid}. The value $V_{gas}/V_{liquid}=1.4$ was used. In this case, as shown in [13], with an initial concentration of SO_2 equal to 1 and 3 vol.%, its equilibrium concentration in the air is equal to 0.001 and 0.008 vol.% at pH in the liquid phase equal to 3.5 and 2.8, respectively. Table 3 shows the corrosion rate of steel and the protective effect of superhydrophobic coatings in the liquid and gas phases in the presence of SO_2 at 1% of the initial concentration.

Table 3. Corrosion rate (K) of steel samples without coating and with SHPCs and their values of the protective effect (Z) in the gas phase (numerator) over a solution of SO_2 (initial concentration is 1%) and liquid phase (denominator) at $V_{gas}/V_{liq}=1.4$ (duration is 10 days).

Type of coating	K, g/(m^2·h)	Z, %
Without coating	0.118/0.058	–
Ni-based SHPC	0.0309/0.0419	73.8/27.8
Zn-based SHPC	0.0084/0.0324	92.9/44.1

From the data presented it follows that the corrosion rate of steel without coating in the gas phase is higher than in the liquid phase, and in the presence of coatings, on the contrary, the resistance of steel in the gas phase is higher, especially in the presence of a zinc-based coating. The protective effect of coatings is higher in the gas phase. The appearance of the coatings was shown to have slight change after the experiment in the gas phase (Figure 7). Point traces of rust were recorded on Zn-based SHPC, and on Ni-based SHPC a rust deposit was observed to a greater extent after exposure to the liquid phase.

The values of contact angles decreased after the experiment in the liquid phase more significantly than after the gas phase, which indicates degradation of the coatings, however, hydrophobicity was preserved, since the contact angles exceeded 90° (Table 4).

Subsequent exposure to air for 42 days contributed to an increase in Θ by only 2 degrees for the samples exposed to the gas phase, and by 1 degree for samples exposed to the liquid phase.

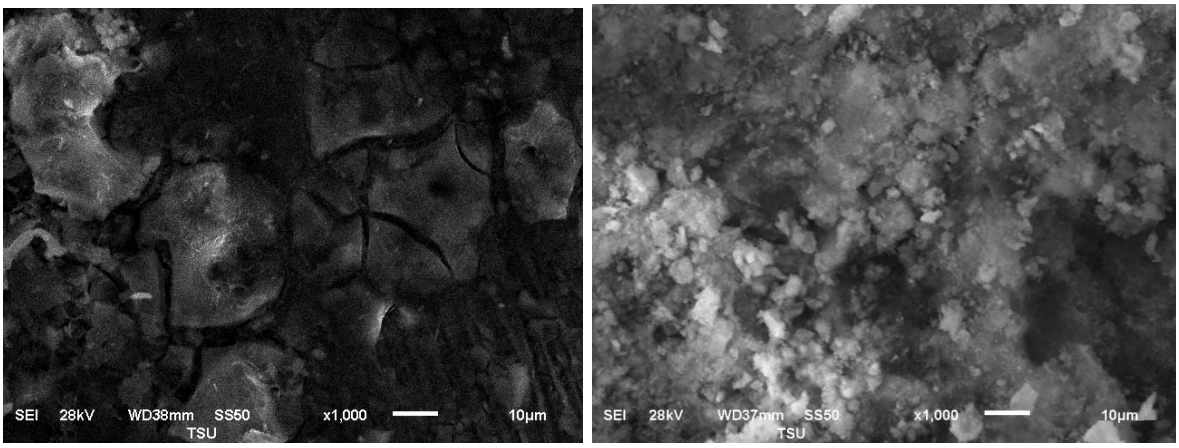

a **b**

Figure 7. SEM image of Ni-based (a) and Zn-based (b) SHP coatings after 10 days of exposure of the samples to the gas phase of a solution with 1% (initial) SO_2.

Table 4. Average values of contact angles on steel plates with a superhydrophobic coating: Θ_1 – initial, Θ_2 – after 10 days in the solution of 1% (initial) SO_2, Θ_3 – after 42 days in air.

Type of coating	Θ_1	Θ_2	Θ_3
Gas phase			
Ni-based SHPC	153.4	130	132.3
Zn-based SHPC	158.2	138.1	140.4
Liquid phase			
Ni-based SHPC	152.7	123.3	124.1
Zn-based SHPC	156.8	128.3	129.3

As the SO_2 concentration increases to 3%, the corrosion rate of steel samples, both uncoated and coated, increases and, accordingly, the protective effect of SHP coatings decreases (Table 5). As with 1% SO_2 concentration, the protective effect of Zn-based SHP coating is higher than that of nickel-based coating.

Contact angles decreased after a 10 day experiment to a greater extent than under conditions of 1% initial SO_2 concentration, especially after exposure to the liquid phase (Table 6, Figure 8).

Table 5. Corrosion rate (*K*) of steel samples without coating and with SHPCs and their values of the protective effect (*Z*) in the gas phase (numerator) over a solution of SO_2 (initial concentration is 3%) and liquid phase (denominator) at V_{gas}/V_{liq}=1.4 (duration is 10 days).

Type of coating	*K*, g/(m²·h)	*Z*, %
Without coating	0.226/0.092	–
Ni-based SHPC	0.0658/0.0726	70.9/21.1
Zn-based SHPC	0.0209/0.0591	90.8/35.8

After exposure to the liquid phase, both types of coatings turned out to be covered with a layer of rust. For Ni-based coatings, the contact angle after exposure to the liquid phase was shown to be less than 90°, and subsequent 42 day exposure to air did not lead to an increase in the angle above 90°. In other cases, the hydrophobicity of the coatings remained unchanged after the experiment; however, subsequent exposure to air contributed to an increase in the contact angles by no more than 1 degree. Apparently, the degradation of the coatings during exposure to SO_2 led to changes that prevent the contact angle from increasing when exposed to air, as it is observed on freshly prepared hydrophobic coatings, where the increase in the angle reaches 8–10 degrees in 2 weeks.

Table 6. Average values of contact angles on steel plates with a superhydrophobic coating: Θ_1 – initial, Θ_2 – after 10 days in the solution of 3% (initial) SO_2, Θ_3 – after 42 days in air.

Type of coating	Θ_1	Θ_2	Θ_3
Gas phase			
Ni-based SHPC	152.1	123.1	124.5
Zn-based SHPC	156.5	131.3	132.4
Liquid phase			
Ni-based SHPC	152.3	87.9	89.1
Zn-based SHPC	157.4	125	126.2

The SEM images of coatings after exposure to the liquid phase of a system with 3% SO_2 shown in Figure 9 indicate a significant change in the state of the Ni-based coating

compared to the original one (Figure 1). The Zn-based coating degraded to a lesser extent. Needle-like structures, in some places in contact with larger particles, obviously determine the retention of hydrophobicity, according to the contact angle values.

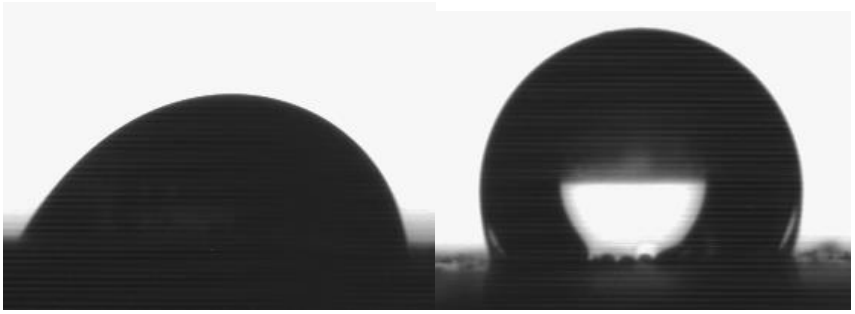

a **b**

Figure 8. Image of water droplets on a Ni-based (a) and a Zn-based (b) SHP coatings after 10 days of holding the samples in the liquid phase of 3% SO_2 solution: a – Θ=87.9°; b – Θ=125°.

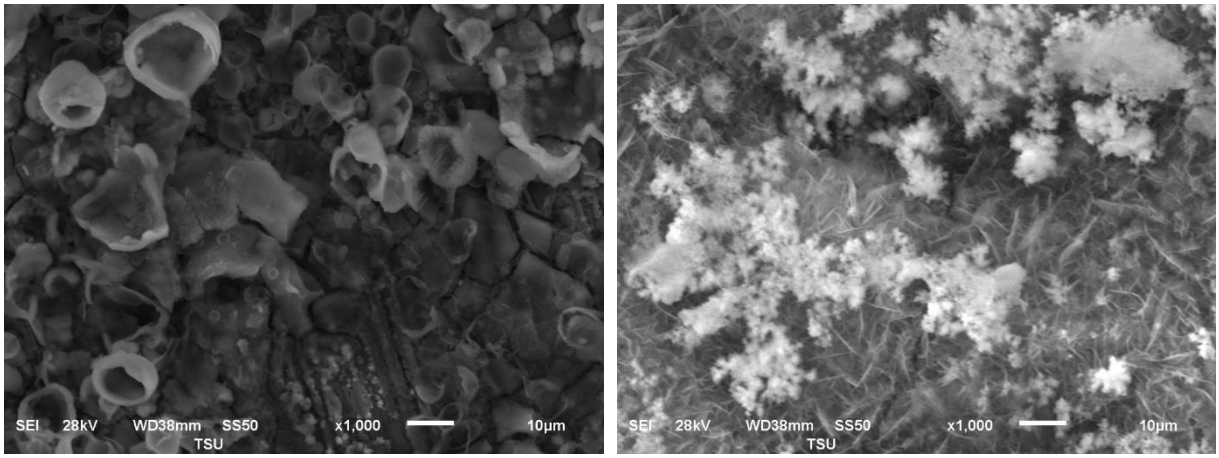

a **b**

Figure 9. SEM image of Ni-based (a) and Zn-based (b) SHP coatings after keeping the samples in the liquid phase of an environment with 3% SO_2.

The protective effectiveness of the superhydrophobic coatings under consideration was also studied in a sodium chloride solution (50 g/L) using the electrochemical methods. Steel samples with SHP coatings were immersed in a saline solution and after a 15-minute exposure, polarization curves (PC) were measured. The samples were kept in the solution for 168 hours and polarization curves were measured every 24 hours. In parallel, measurements were carried out on an steel electrode uncoated. Figure 10 shows PCs measured on the steel electrode without a coating and with two types of coatings at different time intervals of their exposure to a salt environment.

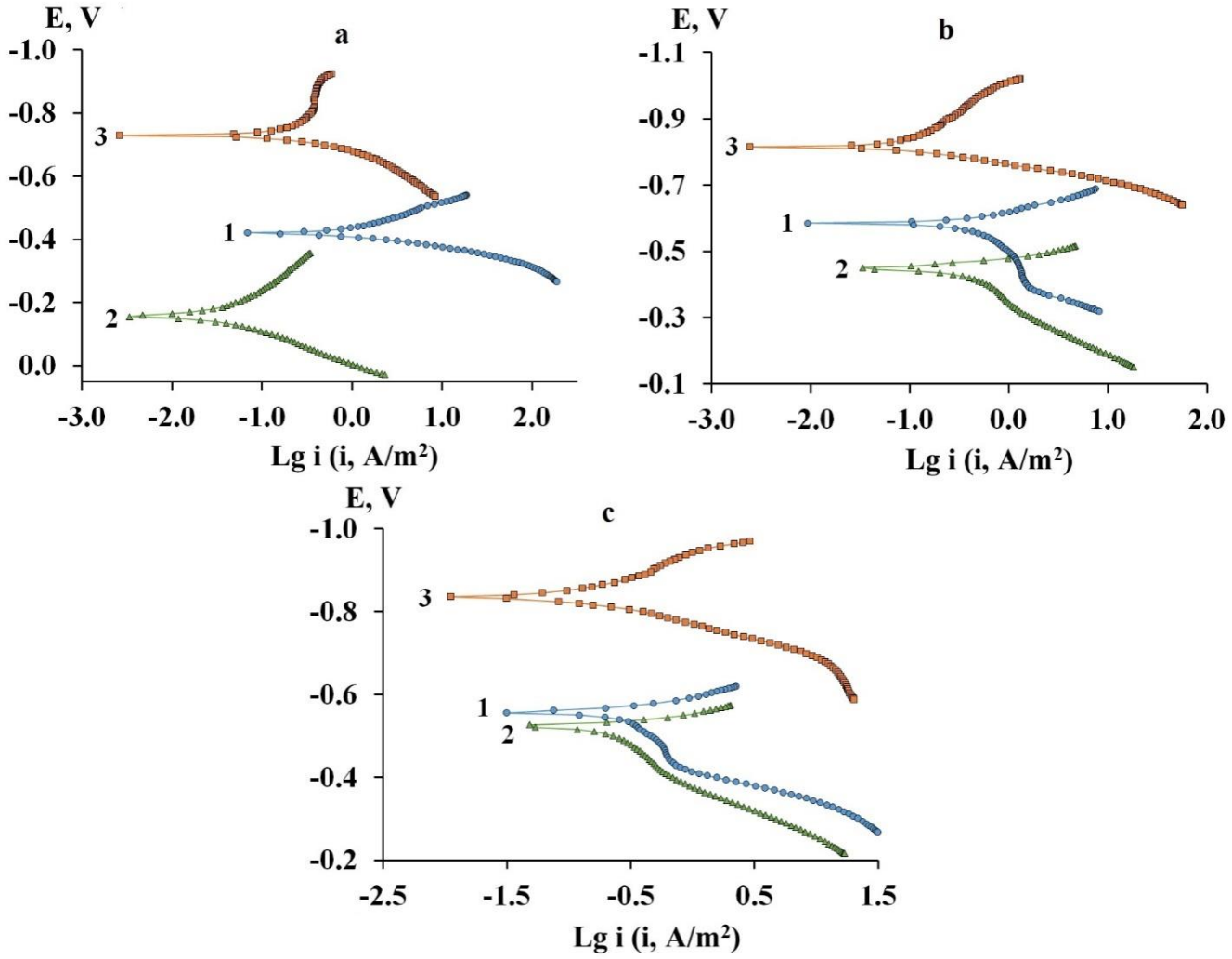

Figure 10. Polarization curves of a steel electrode without coating (1), with Ni-based (2) and Zn-based (3) SHP coatings in a medium of 50 g/L NaCl after exposure, h: a – 0.25; b – 24; c – 168.

After a 15-minute stay in the solution, the corrosion potential E_{cor} of steel without coating is close to –0.42 V, metal corrosion occurs in an active state. The Tafel slope coefficients b_a and b_c are equal to 0.030 and 0.075, respectively, and i_{cor}=0.4196 A/m^2. The E_{cor} of steel with a Ni-based SHP coating 15 min after immersion in the solution is close to –0.160 V with b_a and b_c equal to 0.060 and 0.085 V, respectively, i_{cor}=0.0119 A/m^2. The protective effect *Z* of Ni-based SHPC is 97%, *i.e.*, the corrosion inhibition coefficient is 33.3 (Figure 10a, 1, 2 curves). When comparing curves 1 and 2 in Figure 10a, one can see that in the presence of a Ni-based SHP coating, the anodic reaction is greatly inhibited compared to steel unprotected, with some acceleration of the cathodic process. Corrosion of steel is controlled by the process of anodic ionization.

After 24 hours of exposure to the same environment, the E_{cor} of the electrode without coating decreases to –0.58 V, and that with SHP Ni-based coating, to –0.45 V (Figure 10b, curves 1 and 2). As before, the anodic process on an electrode with SHPC is inhibited and

the cathodic process is facilitated compared to steel unprotected. The i_{cor} of the electrode without coating decreased, while that with the coating increased. This led to a decrease in the *Z* value of the SHP coating to 34%.

Subsequent exposure of the electrodes to the salt environment for 6 days is characterized by E_{cor} fluctuations in the range of (–0.55)…(–0.56) V for a sample unprotected and –(0.46)…(–0.52) V for an electrode with a Ni-based SHP coating (Figure 10c, curves 1 and 2, corresponding to an exposure time in the solution of 168 hours). As before, the anodic process on an electrode coated is inhibited and the cathodic process is facilitated compared to steel unprotected, but the difference in the location of the PCs has significantly decreased compared to the 24-hour situation. At i_{cor}=0.1303 A/m^2 on a steel electrode and 0.1093 A/m^2 on an electrode with coating, the protective efficiency of the SHP coating decreased to 16%, *i.e.*, the corrosion inhibition coefficient is 1.2. We can assume that a steady state has occurred, because the PCs measured after 144 and 168 h coincide.

A completely different picture of the effect on slowing down steel corrosion is observed for Zn-based SHP coatings. After 15 minutes in the solution, the corrosion potential of steel with Zn-based SHPC is equal to –0.73 V, which is 0.31 V more negative than E_{cor} of steel unprotected (Figure 10a, curves 1 and 3). On the cathode branch of the PC there is a section of the limiting current for oxygen equal to 0.38 A/m^2. The value of b_a is 0.040 V, i_{cor}=0.0480 A/m^2. The *Z* value of Zn-based SHPC is 88%, *i.e.* the coating slows down corrosion by 8.3 times. When comparing curves 1 and 3 in Figure 10a, one can see that in the presence of a Zn-based SHP coating, the cathodic reaction is greatly inhibited and the anodic process is facilitated. Corrosion of steel is controlled by the cathodic process.

After 24-hour exposure of the electrodes to the same environment, the E_{cor} of the electrode with a Zn-based coating decreases to –0.82 V, which is 0.24 V more negative than the E_{cor} of the electrode uncoated (Figure 10b, curves 1 and 3). As before, the cathodic process is inhibited on an electrode coated and the anodic process is facilitated compared to steel without coating. i_{cor} of the electrode coated decreased to 0.0436 A/m^2. This led to a decrease in the *Z* value of the Zn-based coating by up to 75%.

Subsequent exposure of the electrodes to a salt environment for 6 days is characterized by fluctuations in the E_{cor} of the electrode with a Zn-based SHP coating in the range of (–0.82)–(–0.85) V. As before, the cathodic process on the electrode coated is inhibited and the anodic process is facilitated compared to the steel one without protect (Figure 10c, curves 1 and 3, corresponding to a holding time in the solution of 168 hours). PCs measured after 144 and 168 hours coincide, indicating the onset of a stationary state. When i_{cor} on the electrode protected is equal to 0.0577 A/m^2, protective effect of the Zn-based coating is equal to 56%.

Thus, the Zn-based SHP coating, although is characterized at the initial stage of exposure to a salt environment by a lesser protective effect than the Ni-based SHP coating, but after 24 hours it shows a better protective effect (75% *vs*. 34%) and, even more so, after 168 hours of exposure (56% *vs*. 16%).

The protective ability of the Zn-based and the Ni-based SHP coatings was also assessed in a salt fog chamber (SFC), in which a 5% NaCl solution was used at a temperature of 35°C

and 100% humidity. The SFC operated in a cyclic manner: each cycle included 1 hour of salt fog spraying and 1 hour with it turned off, after which the cycle was repeated for 8 hours with a complete shutdown with the lid closed for 16 hours. The first signs of corrosion appeared after 28 and 32 hours, respectively, on samples with the Ni-based and the Zn-based SHP coatings, while it took 1 hour on steel samples uncoated. Thus, tests in the SFC also confirmed the better protective effectiveness of Zn-based SHP coatings than those based on Ni.

The results of impedance studies of SHP coatings in the salt solution are shown in Figure 11.

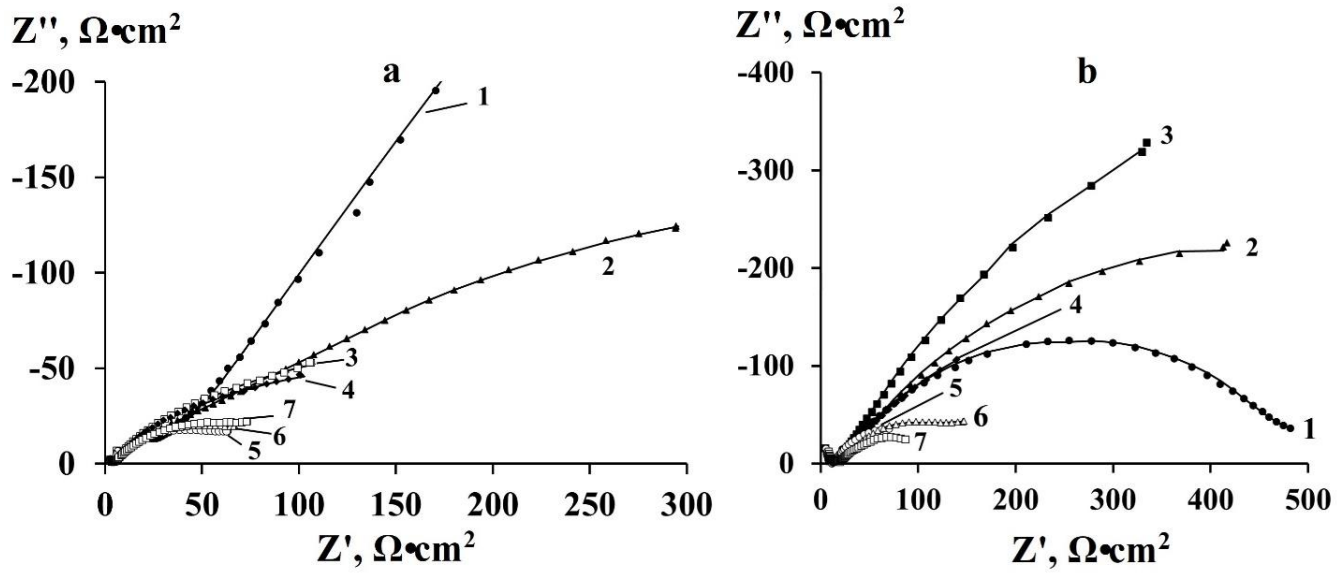

Figure 11. Nyquist diagrams of a steel electrode with Ni-based (a) and Zn-based (b) SHP coatings in a medium of 50 g/L NaCl at E_{cor}. Exposure time of the electrode to the solution, hours: 1 – 0.25; 2 – 24; 3 – 48; 4 – 72; 5 – 96; 6 – 120, 7 – 168.

The points correspond to experimental data, solid lines – to data calculated on the basis of the equivalent circuit in Figure 12.

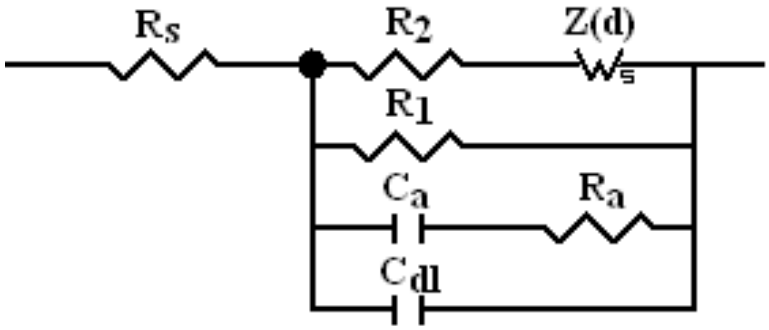

Figure 12. Equivalent circuit simulating the behavior of a steel electrode in test solutions.

In the equivalent circuit of Figure 10, R_1 is the charge transfer resistance of the anodic reaction; the R_a–C_a chain describes the impedance response of the multi-stage iron ionization reaction. The cathodic oxygen reduction process is described by an Ershler–Randles circuit consisting of series-connected resistance R_2 and diffusion impedance Z_d.

For steel samples with a Ni-based SHP coating, the radius of the hodographs decreases with increasing exposure time to the solution, which indicates a decrease in resistance in the system, corresponding to an increase in the corrosion rate (Figure 11). In the case of Zn-based SHP coating, in the first two days the radius of the hodographs increases, and with a further increase in the duration of the experiment it consistently decreases.

Based on the numerical values of the elements of the equivalent circuit (Tables 7, 8), the polarization resistance R_p was calculated using the formula

$$R_p=[R_1\cdot(R_2+R_d)]/(R_1+R_2+R_d) \quad (6)$$

R_p values were used to calculate the protective effect of the SHP coatings:

$$Z,\ \%=100\ (R_{p,SHPC}-R_{p,0})/R_{p,SHPC}, \quad (7)$$

where $R_{p,SHPC}$ and $R_{p,0}$ are the polarization impedance resistance in the presence and absence of SHP coating on steel samples, respectively.

Table 7. Numerical values of elements of the equivalent circuit of the steel electrode with SHP Ni-based coating in 50 g/L NaCl solution.

Element	Duration of sample exposure in solution, hours						
	0.25	**24**	**48**	**96**	**120**	**144**	**168**
R_s, Ω·cm^2	23.6	6.0	2.7	2.8	2.8	3.0	3.2
R_2, Ω·cm^2	68.3	6.0	1.3	1.4	1.7	1.2	1.2
R_d, Ω·cm^2	72481	1083	680.8	670.9	632.7	663	639
τ_d, *s*	36.0	42.1	33.4	29.5	17.7	28.2	27.0
p_d	0.7	0.4	0.5	0.5	0.6	0.5	0.5
R_1, Ω·cm^2	6762	1060	231.1	193.8	77.5	90.8	102.9
C_a, μF/cm^2	2.8	7.4	128.7	124.1	78	128.6	82.7
R_a, Ω·cm^2	67.5	32.7	15.7	13.5	16.3	20.0	25.2
C_{dl}, μF/cm^2	2.5	11.0	37.8	44.2	49.7	62.8	37.7
s, %	3.0	4.3	4.1	4.1	3.9	2.1	3.8
R_p	6185.5	537.2	172.6	150.4	69.1	79.9	88.7
Z, %	98.6	84.1	34.1	19.1	–	16.5	27.7

Table 8. Numerical values of elements of the equivalent circuit of the steel electrode with SHP Zn-based coating in 50 g/L NaCl solution.

Element	Duration of sample exposure in solution, hours						
	0.25	**24**	**48**	**96**	**120**	**144**	**168**
R_s, Ω·cm^2	24	9.9	6.0	7.6	5.7	16.0	12.0
R_2, Ω·cm^2	113.2	15.3	12.7	14.4	8.0	5.7	8.2
R_d, Ω·cm^2	10048	3698	2469	1736	557	1330	414
τ_d, *s*	1.4	211.3	180.6	128.1	154.5	18.5	68.1
p_d	0.6	0.6	0.7	0.6	0.7	0.6	0.6
R_1, Ω·cm^2	475.3	833.2	1769	683.1	130.7	175.1	113.5
C_a, μF/cm^2	14.1	51.8	176	28.5	95.6	18.0	86.8
R_a, Ω·cm^2	128.4	24.7	20.2	18.5	18.1	31.7	22.9
C_{dl}, μF/cm^2	2.3	3.0	44.0	11.7	11.5	15.2	58.9
s, %	3.7	4	4.1	3.9	4.5	2.3	4.2
R_p	454.1	680.5	1032.8	491.3	106.1	154.8	89.5
Z, %	81.3	87.4	89.0	75.2	23.9	56.9	28.4

The values of the protective effectiveness of SHP coatings on steel samples given in Tables 7 and 8 are in satisfactory agreement with the corresponding values calculated on the basis of PCs, especially at the initial and final times of presence of the samples in the solution. Some discrepancies are obviously due to the specific features of impedance measurements.

Conclusions

Superhydrophobic coatings on St3 carbon steel obtained by electrodeposition of nickel and zinc followed by treatment in an ethanol solution of myristic acid are characterized by contact angles of 153±2° and 155±3°, respectively.

SHP coatings showed high resistance when exposed for 240 hours in conditions of 100% humidity and in distilled water, while there were no corrosion lesions, and the contact angles remained virtually unchanged.

With the same duration of stay in the gas and liquid phases of 1 and 3% SO_2 solutions, the SHP coatings degraded somewhat, but retained their hydrophobicity with a protective efficiency in the gas phase ranging from 71–93%. The exception is their presence in the liquid phase of a 3% SO_2 solution, where hydrophobicity has disappeared.

In a NaCl solution (50 g/L), the protective effectiveness of SHP coatings was studied by potentiodynamic polarization and impedance spectroscopy for 168 hours. A high protective effect was shown to be at the initial times of exposure of the samples to the

solution with a gradual decrease over time and preservation of the protective effectiveness towards the end of the stay in the solution.

In all tests, Zn-based coatings showed higher protective effectiveness compared to Ni-based coatings.

Acknowledgment

The results were obtained using the equipment of the Center for Collective Use of Scientific Equipment of TSU named after G.R. Derzhavin. The study was carried out as part of the development program of TSU named after G.R. Derzhavin "Priority-2030".

References

1. A.M. Emelyanenko, F.M. Shagieva, A.G. Domantovsky and L.B. Boinovich, Nanosecond laser micro- and nanotexturing for the design of a superhydrophobic coating robust against long-term contact with water, cavitation, and abrasion, *Appl. Surf. Sci*., 2015, **332**, 513–517. doi: 10.1016/j.apsusc.2015.01.202
2. A. Garcia-Giron, J.M. Romano, Y. Liang, B. Dashtbozorg, H. Dong, P. Penchev and S.S. Dimov, Combined surface hardening and laser patterning approach for functionalising stainless steel surfaces, *Appl. Surf. Sci*., 2018, **439**, 516–524. doi: 10.1016/j.apsusc.2018.01.012
3. T. Xiang, S. Ding, C. Li, S. Zheng, W. Hu, J. Wang and P. Liu, Effect of current density on wettability and corrosion resistance of superhydrophobic nickel coating deposited on low carbon steel, *Mater. Des*., 2017, **114**, 65–72. doi: 10.1016/j.matdes.2016.10.047
4. J. Tan, J. Hao, Z. An and C. Liu, Simple Fabrication of Superhydrophobic Nickel Surface on Steel Substrate via Electrodeposition, *Int. J. Electrochem. Sci*., 2017, **12**, 40–49. doi: 10.20964/2017.01.15
5. H. Gao, S. Lu, W. Xu, S. Szunerits and R. Boukherroub, Controllable fabrication of stable superhydrophobic surfaces on iron substrates, *RSC Adv*., 2015, **5**, 40657–40667. doi: 10.1039/c5ra02890f
6. H. Li, S. Yu, X. Han, S. Zhang and Y. Zhao, A Simple Method for Fabrication of Bionic Superhydrophobic Zinc Coating with Crater-like Structures on Steel Substrate, *J. Bionic Eng*., 2016, **13**, 622–630. doi: 10.1016/S1672-6529(16)60333-5
7. H. Li, S. Yu, J. Hu and X. Yin, Modifier-free fabrication of durable superhydrophobic electrodeposited Cu–Zn coating on steel substrate with self-cleaning, anti-corrosion and anti-scaling properties, *Appl. Surf. Sci*., 2019, **481**, 872–882. doi: 10.1016/j.apsusc.2019.03.123
8. S. Esmailzadeh, S. Khorsand, K. Raeissi and F. Ashrafizadeh, Microstructural evolution and corrosion resistance of SHP electrodeposited nickel films, *Surf. Coat. Technol*., 2015, **283**, 337–346. doi: 10.1016/j.surfcoat.2015.11.005
9. S. Khorsand, K. Raeissi, F. Ashrafizadeh and M.A. Arenas, Relationship between the structure and water repellency of nickel–cobalt alloy coatings prepared by electrodeposition process, *Surf. Coat. Technol*., 2015, **276**, 296–304.

10. L.B. Boinovich, E.B. Modin, A.R. Sayfutdinova, K.A. Emelyanenko, A.L. Vasiliev and A.M. Emelyanenko, Combination of functional nanoengineering and nanosecond laser texturing for design of superhydrophobic aluminum alloy with exceptional mechanical and chemical properties, *ACS Nano*, 2017, **11**, 10113–10123. doi: 10.1021/acsnano.7b04634
11. L.E. Tsygankova, M.N. Uryadnikova, V.I. Kichigin and L.D. Rodionova, Investigation of the corrosion behavior of carbon steel with a protective superhydrophobic coating by impedance spectroscopy method, *Int. J. Corros. Scale Inhib*., 2021, **10**, no. 1, 186–205. doi: 10.17675/2305-6894-2021-10-1-11
12. G.P. Bespamyatnov and Yu.A. Krotov, *Maximum allowable concentrations of chemicals in the environment*, Leningrad, Khimiya, 1985, 528 pp. (in Russian).
13. L.E. Tsygankova, A.A. Uryadnikov, L.D. Rodionova and M.N. Uryadnikova, On the duration of the protective effectiveness of superhydrophobic coatings, *Int. J. Corros. Scale Inhib*., 2023, **12**, no. 3, 1211–1223. doi: 10.17675/2305-6894-2023-12-3-23

♦ ♦ ♦